ARTICLE OPEN

Check for updates

# Regulation of craving and underlying resting-state neural circuitry predict hazard of smoking lapse

Spencer Upton [1]✉ and Brett Froeliger[1,2]



Among individuals with substance use disorders, clinical outcomes may be improved by identifying brain-behavior models that predict drug re/lapse vulnerabilities such as the ability to regulate drug cravings and inhibit drug use. In a sample of nicotine-dependent adult cigarette smokers ($N = 213$), this laboratory study examined associations between regulation of craving (ROC) efficacy and smoking lapse, utilized functional connectivity multivariate pattern analysis (FC-MVPA) and seed-based connectivity (SBC) analyses to identify resting-state neural circuitry underlying ROC efficacy, and then examined if the identified ROC-mediated circuitry predicted hazard of smoking lapse. Regarding behavior, worse ROC efficacy predicted a greater hazard of smoking lapse. Regarding brain and behavior, FC-MVPA identified 29 brain-wide functional clusters associated with ROC efficacy. Follow-up SBC analyses using 9 of the FC-MVPA-derived clusters identified a total of 64 resting-state edges (i.e., cluster-to-cluster connections) underlying ROC efficacy, 10 of which were also associated with the hazard of smoking lapse. ROC efficacy edges also associated with smoking lapse were largely composed of connections between frontal-striatal-limbic clusters and sensory-motor clusters and better behavioral outcomes were associated with stronger resting-state FC. Findings suggest that both ROC efficacy and underlying resting-state neural circuitry may inform prediction models of re/lapse vulnerabilities and serve as treatment targets for cessation interventions.

*Translational Psychiatry* (2025)15:101 ; https://doi.org/10.1038/s41398-025-03319-1

## INTRODUCTION

Expanding on examinations into craving in addiction [1–4], recent efforts have begun examining the proactive regulation of craving (ROC: the ability to dampen motivational responses to drug-related cues via cognitive reappraisal) [5–17]. The extant literature, which is exclusively based on the hypothesis-driven task-based fMRI blood-oxygenation-level-dependent (BOLD) assessment of ROC, suggests activity in frontal-striatal-limbic circuitry mediates ROC efficacy [7]. Specifically, these studies show increased activations in left-lateralized prefrontal circuitry (inferior, middle, superior frontal gyrus), concomitant with decreased activations in striatal-limbic circuitry (caudate, amygdala, subgenual cingulate, medial orbital gyrus) [17, 18]. However, a recent data-driven investigation into the BOLD assessment of craving and its regulation found that behavior was best predicted by whole-brain BOLD effects, including fronto-striatal-limbic circuitry, sensory-motor circuitry, and temporal-parietal circuitry [19], thus expanding on current knowledge.

Although much is known about what brain regions are important for ROC efficacy as assessed via BOLD response, an absence of knowledge remains surrounding how these brain regions communicate with one another as assessed via BOLD functional connectivity [20] (e.g., resting-state FC [rsFC]), and how these neural mechanisms are associated with clinical outcomes such as drug re/lapse. Specifically, no studies to the best of our knowledge have examined associations between ROC efficacy and rsFC, ROC efficacy and drug re/lapse, or ROC efficacy-mediated rsFC and drug re/lapse. Furthermore, the majority of the mechanistic work conducted thus far has been restricted to underpowered hypothesis-driven task-based BOLD response methods, which is an approach with significant limitations [21]. Thus, there is a critical need for an integrated and adequately-powered data-driven examination of ROC efficacy, BOLD FC, and drug re/lapse to extend current knowledge and elucidate novel mechanisms underlying re/lapse vulnerabilities.

rsFC research has grown dramatically over the past decade due to its success in informing models of addiction pathophysiology, which is the result of multiple factors including its feasibility, accessibility, and due to the fact that, as a function of how the data are modeled (only have one condition – rest), it has more desirable psychometric properties (test-retest reliability) as compared to methods which seek to model multiple conditions [21, 22]. Regarding rsFC models on individuals with nicotine dependence, weakened rsFC [23–31] between the inferior frontal gyrus / insula and striatal-limbic circuitry has been consistently associated with an increased risk for smoking behaviors. Moreover, this working model has been bolstered by research observing these same patterns in task-based FC studies [25, 31, 32], as well as by recent transcranial magnetic stimulation research demonstrating that stimulating the inferior frontal gyrus can strengthen fronto-striatal-limbic rsFC and correspondingly reduce craving and smoking [33, 34].

[1]Department of Psychological Sciences, University of Missouri, Columbia, MO, USA. [2]Department of Psychiatry, University of Missouri, Columbia, MO, USA.
✉email: uptons@missouri.edu

Received: 15 August 2024 Revised: 22 February 2025 Accepted: 14 March 2025
Published online: 28 March 2025

However, despite progress, the addiction field's hypothesis-driven focus on frontal-striatal-limbic circuitry has potentially limited the elucidation of other important circuitry underlying re/lapse vulnerabilities and thus other important treatment targets for clinical intervention, as suggested by recent research [19]. Thus, one crucial step forward is to utilize data-driven methods and provide comparisons with hypothesis-driven findings reported in the literature. Regarding rsFC research, one novel data-driven approach gaining popularity is functional connectivity multivariate pattern analysis (FC-MVPA) [35–40], which is a spatiotemporal multivariate method for identifying patterns of FC that underly a given behavior. Simply, FC-MVPA procedures include: decomposing FC data into voxel-specific orthogonal components that maximize intersubject heterogeneity; regressing the components onto a variable of interest to identify functional clusters displaying multivariate patterns of FC associated with the variable of interest; and finally, using the FC-MVPA-derived clusters as seed regions for follow-up seed-based connectivity (SBC) analyses on the original data to identify edges (i.e., cluster-to-cluster connections) associated with the variable of interest. Explicit benefits of FC-MVPA include being better suited to detect weaker multivariate whole-brain effects and not being restricted to a priori specified atlas parcellations [35].

In this laboratory study, sated nicotine-dependent adults who smoke cigarettes ($N = 213$) completed a resting-state fMRI scan and then immediately following and outside of the scanner, completed a smoking relapse analog task (SRT) [41–43], which assessed ROC efficacy, latency inhibiting smoking, and smoking lapse. The goal of this study was to examine if ROC efficacy and underlying resting-state neural circuitry, could respectively, predict a laboratory assessment of smoking lapse. Specifically, this study examined associations between ROC efficacy and smoking lapse, utilized FC-MVPA procedures to identify neural circuitry underlying ROC efficacy, and then examined if the identified ROC-mediated rsFC circuitry predicted smoking lapse. ROC efficacy edges also associated with smoking lapse were of primary interest. Although the study relied on a data-driven approach, it was hypothesized that (1) worse ROC efficacy would be associated with greater hazard for smoking lapse; and based on the extant literature [17, 18], that (2) ROC efficacy would be associated with left-lateralized prefrontal functional clusters, fronto-striatal-limbic edges, and that stronger fronto-striatal-limbic ROC-mediated rsFC would be associated with better SRT outcomes. However, based on recent knowledge [19], we anticipated observing important effects outside of fronto-striatal-limbic circuitry.

## MATERIALS AND METHODS

### Participants

Study analyses pooled data from adults ($N = 213$; 54.9% female: $M_{age} = 43.6 \pm 11.06$; age range: 21–69) who smoked an average of 17 cigarettes per day (CPD) ($M_{CPD} = 17.4 \pm 6.5$; range: 4–40) for an average of 26 years ($M_{years} = 25.6 \pm 11.8$; range: 3–53) (Table 1). Inclusion criteria were being aged 18–70 years; English fluency; functional vision; and being a current nicotine-dependent cigarette smoker for at least the last two years. Exclusion criteria included a self-reported history of unstable mental or physical health (current or past psychosis; or having an untreated medical or psychiatric condition); history or MRI evidence of a neurological disorder; contraindication to MRI; use of smoking cessation medications in the last month; positive pregnancy test; or breath alcohol content >0. Data were collected from IRB-approved protocols at the University of Missouri −Columbia and the Medical University of South Carolina. Participants gave written informed consent and received financial compensation for participation. Separate from money earned during the smoking relapse analog task (SRT), participants received an average of $135 (range: $110–$160) for completing the study protocol outlined here.

### Study design

All participants completed an initial screening and training visit which included an MRI mock scan and training on the SRT. SRT training entailed completing at least one block of the task under the supervision of research staff, and if needed, additional training was provided until each participant understood task instructions. All participants included in analyses demonstrated comprehension and the ability to perform the task during training. On a separate day, participants returned for a laboratory experimental visit while smoking satiated that included MRI scanning (1 h) and then performing the SRT (1 h).

**Table 1.** Participants.

| Measure | Participants ($N = 213$) |
|---|---|
| Demographics | |
| Sex, female, n (%) | 117 (54.9%) |
| Sex, male, n (%) | 96 (45.1%) |
| Age, years, mean (SD) | 43.62 (11.06) |
| Education, years, mean (SD) | 14.14 (2.30) |
| Race, n (%) | |
| Caucasian non-Latinx/Hispanic | 165 (77.5%) |
| Black or African American | 37 (17.4%) |
| Multiple | 10 (5%) |
| Not reported | 1 (0.1%) |
| Household Income, Annually, n (%) | |
| $16,000 or less | 42 (19.7%) |
| $16,001–31,000 | 38 (17.8%) |
| $31,001–48,000 | 39 (18.3%) |
| $48,001–64,000 | 31 (14.6%) |
| $64,001–80,000 | 22 (10.3%) |
| $80,001–96,000 | 16 (7.5%) |
| $96,001 or more | 20 (9.4%) |
| Not reported | 5 (2.4%) |
| Clinical Characteristics, mean (SD) | |
| Nicotine dependence, FTND | 5.41 (1.89) |
| Breath carbon monoxide (CO), mean ppm (SD) | 23.82 (11.94) |
| Craving, QSUB | 32.37 (15.47) |
| Cigarettes per day (CPD), past 30 days | 17.41 (6.54) |
| Years smoking | 25.58 (11.80) |
| Pack years | 23.15 (15.21) |
| Depressive symptoms, CES-D | 14.51 (8.99) |
| Anxiety symptoms, BAI | 5.31 (7.04) |
| Smoking Relapse Analog Task (SRT) | |
| Regulation of craving (ROC) efficacy, mean (SD) | −0.68 (1.17) |
| Latency inhibiting smoking, mean (SD) | 7.81 (3.05) |
| Smoking lapse, n (%) | 86 (40.4%) |

*FTND* fagerström test for nicotine dependence (range: 0–10), *ppm* parts per million, *QSUB* questionnaire of smoking urges brief (range: 10–70), *CES-D* center for epidemiological studies-depression (range: 0–60), *BAI* beck anxiety inventory (range: 0–63).

### Smoking relapse analog task (SRT)

Following the MRI, participants performed the SRT outside of the scanner. While seated at a computer desk in a ventilated room, participants were provided with an open pack of their preferred brain of cigarettes, an ashtray, and a lighter at arm's reach. In 6 min. blocks, for up to 10 blocks, participants performed the Regulation of Craving (ROC) task (See below). After each block, participants were given the option to either continue the task smoke-free and earn additional money ($1 per block completed), or they could quit the task and freely smoke (lapse) in the same ventilated room. All participants were required to complete at least 1 block. To

encourage participants to perform the task to their best ability, participants were informed that regardless of when they quit the task, they would remain in the room for the entire 60 min. period. As discussed below, the SRT [41–43] assessed three smoking-related behaviors: ROC efficacy [7, 44], latency inhibiting smoking [45, 46], and smoking lapse (Fig. S1).

*ROC task*. While participants viewed smoking-related images, the instruction of either "Now" or "Later" was presented. During "Smoke Now [SN]" trials, participants were instructed to contemplate the immediate experience of what it would feel like to smoke now (e.g., pleasurable sensations from smoking). During "Smoke Later [SL]" trials, participants were instructed to contemplate the long-term negative consequences of smoking (e.g., adverse health outcomes). Participants also viewed neutral non-smoking images (e.g., pencil, towel) while being presented with the instruction "Look." During "Neutral Look [NL]" trials, participants were instructed to look at the image without using any strategies. After each trial, participants rated their level of craving on a scale from 1 (no craving) to 8 (extreme craving). ROC efficacy scores were calculated (SL – SN) and used for later analyses. Negative scores indicated greater success with regulating craving. Each of the three conditions were randomly presented 8 times in each block. Trials included the following sequence: instruction (2 s), cue (6 s), crave rating (3 s), and fixation point (jittered mean on 3 s).

*Latency inhibiting smoking*. Participants received $1 for each 6 min. block they completed and could do this for up to 10 blocks (could earn $1–$10 over the course of 6–60 min.). The number of blocks completed (time on task) was used for later analyses.

*Smoking lapse*. If participants failed to complete all 10 blocks, thus opting to quit and smoke, this was coded as a smoking lapse event (binary outcome: 0 = no; 1 = yes) and used for later analyses.

## MRI details and analyses

All MRI analyses were performed using the CONN toolbox [47] and SPM [48] in MATLAB. In sum, FC-MVPA procedures were conducted on cleaned rsFC data to identify neural circuitry (functional clusters via FC-MVPA and edges via SBC) associated with ROC efficacy. For information on image acquisition, preprocessing, denoising, and quality control, see Supplemental Text and Fig. S2.

*FC-MVPA (step 1)*. First, FC-MVPA [35] was performed to estimate the first 21 eigenpatterns characterizing the principal axes of heterogeneity in rsFC across subjects. Next, 21 eigenpattern-score images were derived for each subject (10:1 ratio of subjects-to-components), characterizing their brain-wide functional connectome state (Table S1). Eigenpatterns and eigenpattern-scores were computed separately for each voxel as the left- and right-singular vectors, respectively, from a singular value decomposition (group-level SVD) of the matrix of FC values between a given voxel and the rest of the brain (a matrix with one row per target voxel, and one column per subject). Individual FC values were then computed from the matrices of bivariate correlation coefficients between the BOLD timeseries from each pair of voxels, estimated using an SVD of the z-score normalized BOLD signal with 64 components separately for each subject (subject-level SVD). In sum, step 1 reduced the dimensionality of the data to a set of components that retained a large amount of the data's variance.

*ROC efficacy FC-MVPA (step 2)*. Next, a group-level multivariate general linear model (GLM) using the 21 eigenpattern-score images was built and assessed whether there was any effect of ROC efficacy across the voxel-to-voxel connectome after adjusting for the effects of scanner, mean framewise displacement, age, and sex. Cluster-level inferences were based on nonparametric statistics using 1000 permutations, an uncorrected voxel-level threshold of $p < 0.005$, and an FDR-corrected cluster-mass threshold of $p < 0.05$. In sum, step 2 used the first 21 components in a regression analysis to identify functional clusters associated with ROC efficacy.

*ROC efficacy SBC analyses (step 3)*. Lastly, multiple group-level multivariate GLMs, using the original rsFC seed-to-voxel maps for a given ROC efficacy FC-MVPA-derived cluster, were built and performed. The question these analyses asked was, from a given ROC efficacy FC-MVPA seed cluster, where in the connectome and in what direction was rsFC associated with ROC efficacy after adjusting for the effects of scanner, mean framewise displacement, age, and sex. Since the prior step identifies clusters known to have ROC efficacy edges, nonparametric cluster-level inferences here utilized a more conservative threshold to adjust for this bias which included 1000 permutations, an uncorrected voxel-level threshold of $p < 0.001$, and an FDR-corrected cluster-mass threshold of $p < 0.05$. In sum, step 3 used the previously derived clusters as seed regions in SBC regression analyses on the original rsFC data to identify edges (cluster-to-cluster connections) associated with ROC efficacy. ROC efficacy edge rsFC (Fisher-transformed bivariate correlation coefficients [rZ values]) were extracted and used for further analyses.

*rsFC composite score*. In addition to examining brain-behavior associations using individual edge rsFC, this study also examined the effects of rsFC composite scores. Composite score calculations were based on a well-established procedure [49–54] that collapses rsFC values from multiple edges into single scalar values (i.e., combined edge strength). Composite scores have been shown to explain more variance and display higher test-retest reliability [54], and thus have greater biomarker potential (Supplemental Text). Here, a composite score was calculated for ROC edges also found to be associated with smoking lapse and was used in follow-up analyses.

## Additional details and analyses

Additional analyses took place in SPSS (version 28) and JASP (version 0.19.2). Descriptive statistics were performed to characterize performance on the SRT and edge rsFC. A one-way repeated measures ANOVA was used to confirm differences in craving to the three conditions on the ROC task. Cox regression survival analyses were conducted to separately examine associations between ROC efficacy and ROC efficacy-mediated rsFC on smoking lapse. Since analyses between rsFC and smoking lapse were exploratory, multiple comparisons correction was not used. For descriptive purposes, k-means clustering (k = 2) was separately applied to ROC efficacy (better vs. worse) and ROC efficacy-mediated rsFC (stronger vs. weaker) to display group differences in smoking lapse survival curves. Lastly, exploratory robustness analyses (Tables S2–4) were conducted to examine the effects of covariates and between-subject factors on study outcomes; and post-hoc cross-validation analyses (Table S5–6) were conducted on brain-behavior associations to assess predictive effects based on random sampling variability. Box plots, histograms, Cox regression plots, Kaplan-Meier plots, and partial regression plots were used to visualize study outcomes. Statistical significance was defined as $p < 0.05$ (two-tailed). Data distributions were assumed to be normal. No power analyses were conducted to predetermine sample size.

# RESULTS

## Behavior

*ROC task*. There was a significant effect of condition on craving ($F_{2,211} = 100.223$, $p < 0.001$, $np^2 = 0.487$). Follow-up comparisons revealed that all conditions (NV: M = 3.56, SD = 1.84; SN: M = 5.04, SD = 2.03; SL: M = 4.36, SD = 2.00) were significantly different from each other. Specifically, craving for NV was lower than craving for SN ($M_{diff} = -1.47$, SE = 0.11, 95% CI = −1.69 to −1.26, $p < 0.001$, $np^2 = 0.464$) and SL ($M_{diff} = -0.79$, SE = 0.11, 95% CI = −1.02 to −0.573, $p < 0.001$, $np^2 = 0.192$). Also, craving for SL was lower than craving for SN ($M_{diff} = -0.68$, SE = 0.08, 95% CI = −0.838 to −0.521, $p < 0.001$, $np^2 = 0.252$), confirming participants were downregulating their cigarette cravings via cognitive reappraisal (ROC: M = −0.68, SD = 1.17) (Fig. 1A).

*Latency inhibiting smoking*. The mean duration participants inhibited from smoking was 7.81 (SD = 3.05) blocks (47 min.) (Fig. 1B).

*Smoking lapse*. 86 participants (40%) experienced a smoking lapse event, while 127 (60%) abstained from smoking over the entire 60 min. duration (Fig. 1B).

*Association between ROC efficacy and smoking lapse*. Worse ROC efficacy was associated with a greater hazard of smoking lapse (β = 0.257, SE = 0.121, HR = 1.294, 95% CI = 1.020–1.641,

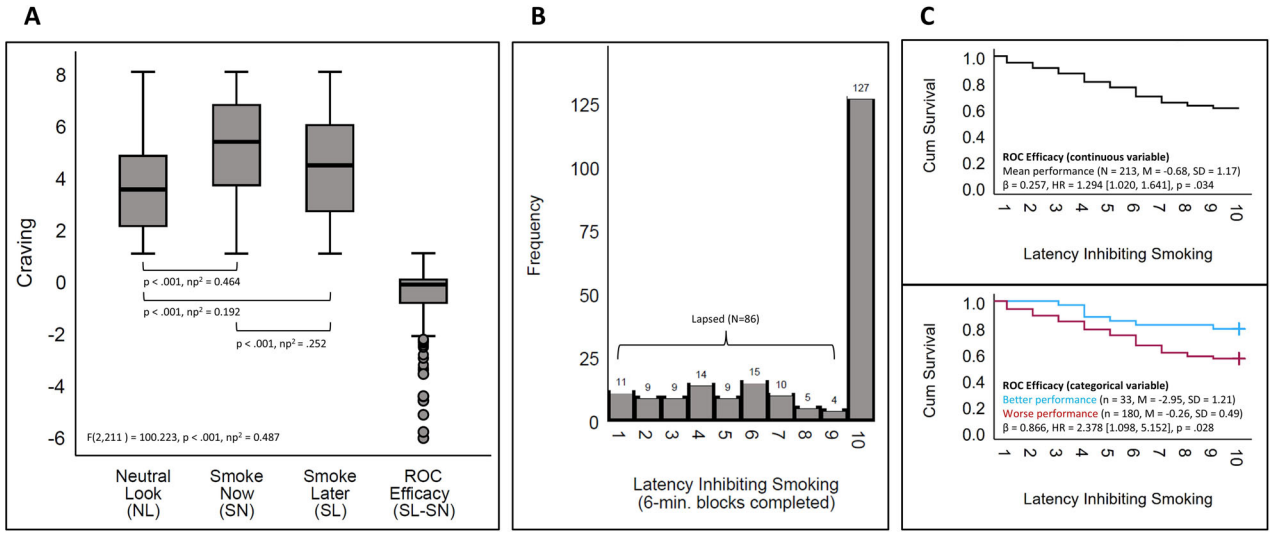


**Fig. 1 Behavioral results.** (**A**) There was a significant effect of condition on craving ($F_{2,211} = 100.223$, $p < 0.001$). Comparisons revealed that all conditions (NV: M = 3.56, SD = 1.84; SN: M = 5.04, SD = 2.03; SL: M = 4.36, SD = 2.00) were statistically different. Importantly, craving for SL was lower than craving for SN ($M_{diff} = -0.68$, $p < 0.001$), demonstrating participants could downregulate their cigarette cravings (ROC: M = −0.68, SD = 1.17). (**B**) On average, participants inhibited smoking for 7.81 (SD = 3.05) blocks, and 86 (40%) experienced a smoking lapse event. (**C top**) Worse ROC efficacy was associated with a greater hazard of smoking lapse (β = 0.257, HR = 1.294, $p = 0.034$). Specifically, for every one-unit increase in ROC efficacy (the more positive the value, the worse the performance), there was a 29% increase in the hazard of smoking lapse. (**C bottom**) For descriptive purposes, k-means clustering (k = 2) was applied to ROC efficacy to display differences in survival curves based on group task performance (better vs. worse). Worse performers exhibited a greater hazard of smoking lapse (β = 0.866, HR = 2.378, $p = 0.028$). Statistical significance: $p$-value < 0.05 (two-tailed).

$p = 0.034$). Specifically, for every one-unit increase in ROC efficacy (positive values indicate worse performance), there was a 29% increase in the hazard of smoking lapse (Fig. 1C [**top**]). No time-dependent effect of ROC efficacy on smoking lapse was found ($p = 0.377$) suggesting the proportional hazards assumption was met. For descriptive purposes, k-means clustering (k = 2) was applied to ROC efficacy to display differences in survival curves based on group task performance (better [$N = 33$; M = −2.95, SD = 1.21] vs. worse [$N = 180$; M = −0.26, SD = 0.49]). Follow-up descriptive analyses indicated that individuals with worse performance exhibited greater hazard of smoking lapse (β = 0.866, SE = 0.394, HR = 2.378, 95% CI = 1.098–5.152, $p = 0.028$) (Fig. 1C [**bottom**]).

## Brain and behavior

*ROC efficacy FC-MVPA.* In sum, analyses identified 29 functional clusters associated with ROC efficacy, which spanned left-lateralized prefrontal circuitry, striatal-limbic circuitry, temporal-parietal circuitry, and sensory-motor circuitry (Fig. 2). 9 clusters were selected for follow-up SBC analyses in order to identify edges underlying ROC efficacy. Cluster selection was informed by the ROC efficacy BOLD response literature [7, 17–19], prevailing addiction neuroscience models [55, 56], and reasons regarding our hypotheses. Although the selected clusters spanned multiple regions (especially cluster one), peak regions for each included the: right anterior cingulate; left medial orbital gyrus; left inferior frontal gyrus; right dorsal striatum; left lateral orbital gyrus; right amygdala; right anterior insula; left middle frontal gyrus; and left pre-supplemental motor area (Supplemental Text; Tables S7).

*ROC efficacy SBC analyses and associations with smoking lapse.* In sum, follow-up SBC analyses from the 9 selected FC-MVPA clusters identified 64 edges underlying ROC efficacy. Of these 64 edges, 10 also predicted the hazard of smoking lapse (Fig. 3; Table 2). The results are briefly described below (Supplemental Text; Tables S8−9).

Anterior cingulate / Middle frontal gyrus / Parietal lobule seed cluster edges: The first selected cluster spanned numerous regions including the bilateral pregenual cingulate gyrus, left anterior middle frontal gyrus, left frontal pole, bilateral middle cingulate gyrus, right inferior parietal lobule, right postcentral gyrus, and the bilateral paracentral lobule. Although ROC efficacy edges were found (Fig. 3), none predicted smoking lapse.

Medial orbital gyrus seed cluster edges: The second selected cluster spanned the left and right medial orbital gyrus. Although ROC efficacy edges were found (Fig. 3), none predicted smoking lapse.

Left inferior frontal gyrus seed cluster edges: The third selected cluster spanned the left inferior frontal gyrus pars triangularis, pars opercularis, and dorsal anterior insula. Analyses identified 4 ROC efficacy edges that were also associated smoking lapse. Specifically, stronger rsFC from this cluster to the right precentral gyrus and supplementary motor area, left precentral gyrus, right postcentral gyrus, and left paracentral lobule were each associated with better ROC efficacy and less hazard for smoking lapse (Fig. 3, Table 2). An additional 2 ROC efficacy edges from this cluster displaying notable associations with smoking lapse spanned connections to striatal-thalamic regions ($p = 079$; $p = 0.117$).

Right dorsal striatum seed cluster edges: The fourth selected cluster spanned the right dorsal caudate, globus pallidus, and putamen. Analyses identified 1 ROC efficacy edge that was also associated with smoking lapse. Specifically, stronger rsFC from this cluster to the right dorsal anterior insula and inferior frontal gyrus pars opercularis was associated with better ROC efficacy and less hazard for smoking lapse (Fig. 3, Table 2).

Left lateral orbital gyrus seed cluster edges: The fifth selected cluster spanned the left lateral orbital gyrus. Although ROC efficacy edges were found (Fig. 3), none predicted smoking lapse. However, 2 ROC efficacy edges from this cluster displaying notable associations with smoking lapse spanned connections to the precentral gyrus and middle frontal gyrus ($p = 0.099$; $p = 0.104$).

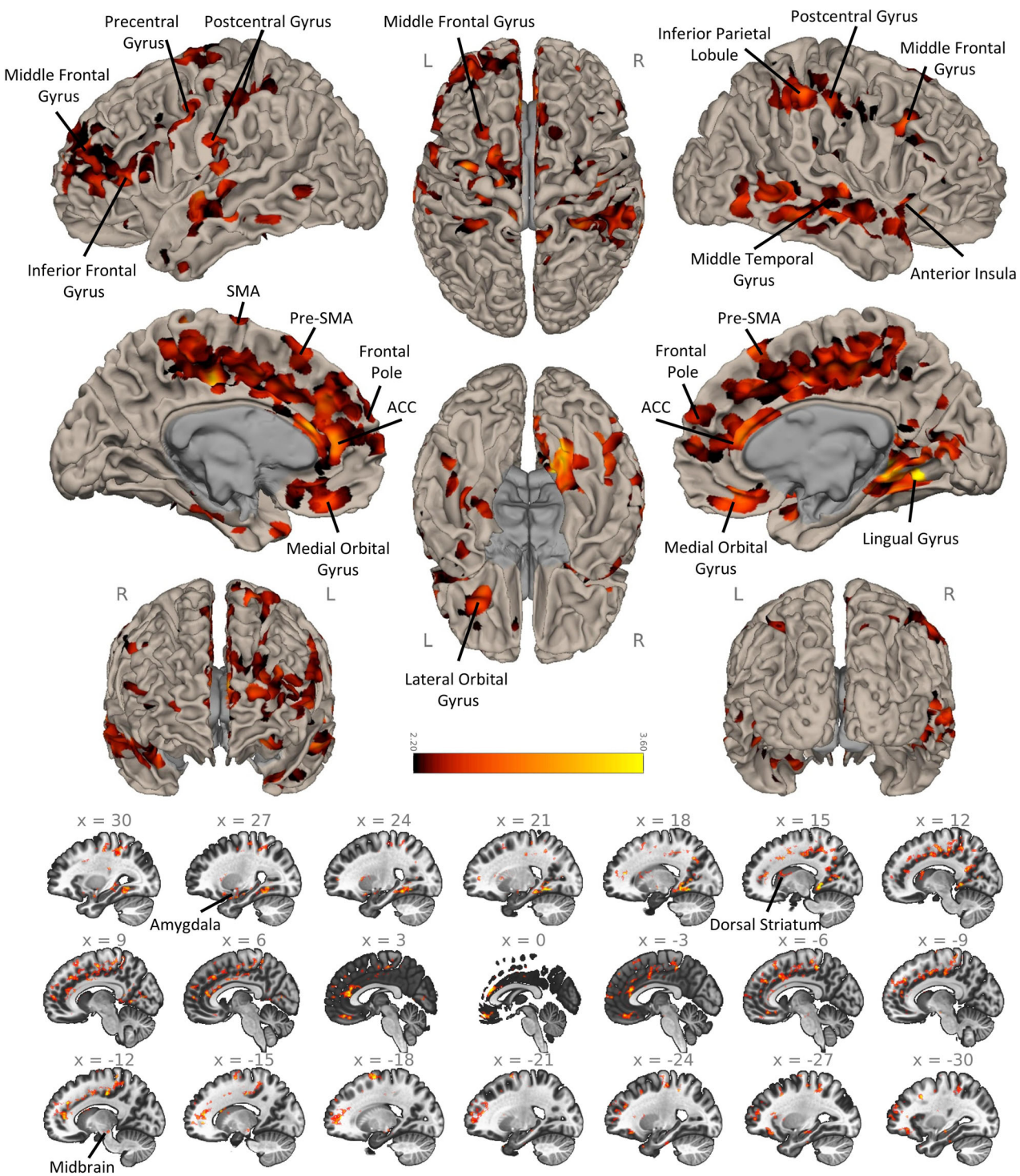


**Fig. 2 Brain-behavior results: ROC Efficacy FC-MVPA.** A group-level multivariate general linear model (GLM) using 21 eigenpattern-score images was built and assessed whether there was any effect of ROC efficacy across the voxel-to-voxel connectome after adjusting for the effects of scanner, mean framewise displacement, age, and sex. Volumetric results are displayed on the projected cortical surface (top) and in Montreal Neurological Institute (MNI) space (bottom). Analyses identified 29 functional clusters displaying multivariate patterns of resting-state functional connectivity (rsFC) associated with ROC efficacy. Clusters spanned left-lateralized prefrontal circuitry, striatal-limbic circuitry, temporal-parietal circuitry, and sensory-motor circuitry. Statistical significance: 1000 permutations, uncorrected voxel-level threshold of $p < 0.005$, and FDR-corrected cluster-mass threshold of $p < 0.05$.

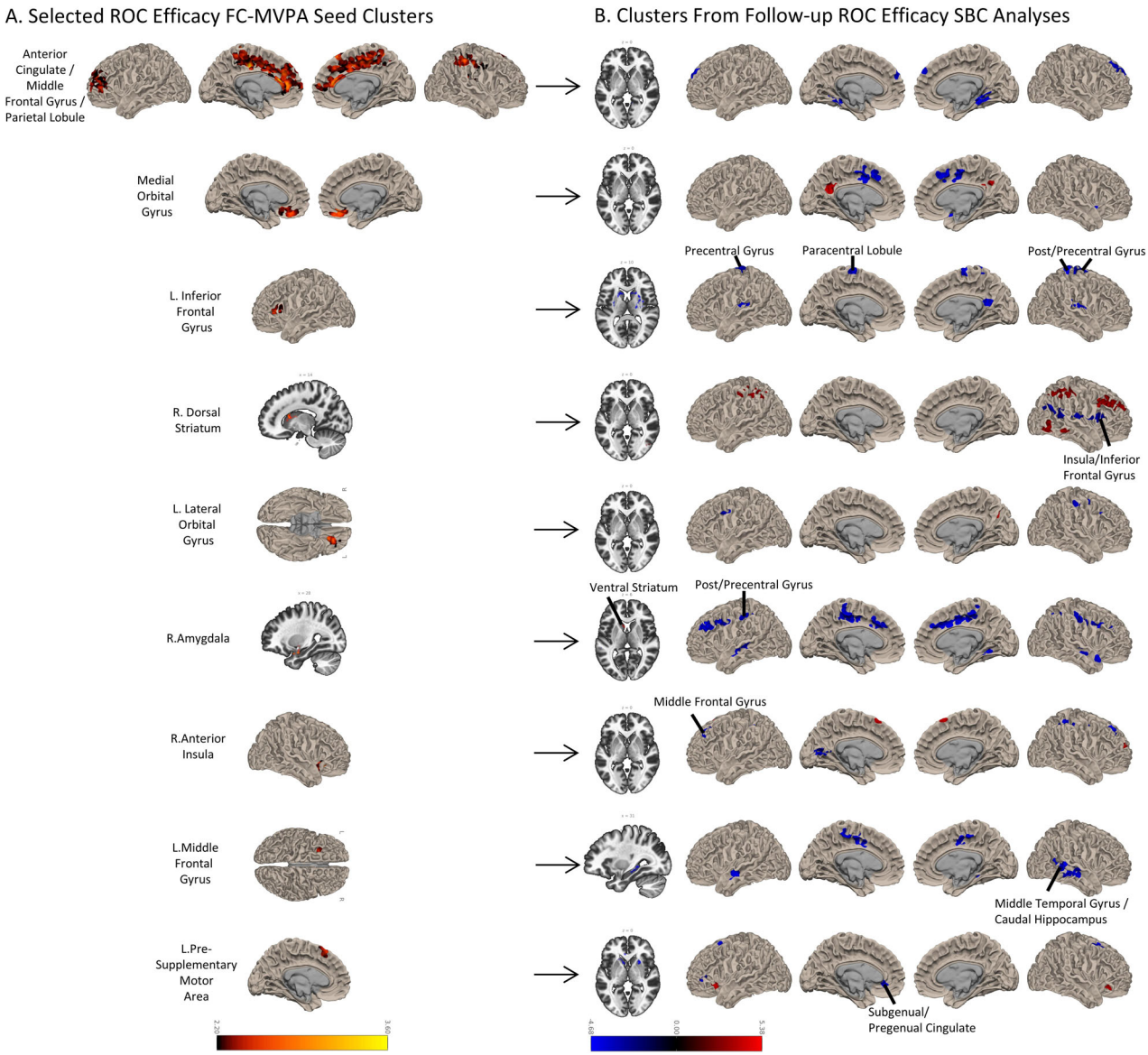


**Fig. 3 Brain-behavior results: ROC Efficacy SBC analyses and associations with smoking lapse.** Multiple group-level multivariate general linear models (GLMs), using the original rsFC seed-to-voxel maps for a given ROC efficacy FC-MVPA-derived cluster, were built and performed. The question these analyses asked was, from a given ROC efficacy FC-MVPA-derived cluster, where in the connectome and in what direction was rsFC associated with ROC efficacy after adjusting for the effects of scanner, mean framewise displacement, age, and sex. **A** Depicts the selected ROC efficacy FC-MVPA seed clusters. **B** Depicts the resulting ROC efficacy SBC clusters. ROC efficacy edges (cluster-to-cluster connections) also associated with smoking lapse are labeled in the figure and characterized in Table 2. Statistical significance: 1000 permutations, uncorrected voxel-level threshold of $p < 0.001$, and FDR-corrected cluster-mass threshold of $p < 0.05$ [exception was dorsal striatum (voxel-level threshold was $p < 0.05$)].

Right amygdala seed cluster edges: The sixth selected cluster spanned the right lateral and medial amygdala. Analyses identified 2 ROC efficacy edges also associated with smoking lapse. Specifically, weaker rsFC from this cluster to the left ventral caudate, yet stronger rsFC from this cluster to the left postcentral and precentral gyrus were each associated with better ROC efficacy and less hazard for smoking lapse (Fig. 3, Table 2). An additional ROC efficacy edge from this cluster displaying notable associations with smoking lapse spanned a connection to the left middle cingulate gyrus and precentral gyrus ($p = 0.094$).

Right anterior insula seed cluster edges: The seventh selected cluster spanned the right ventral anterior insula and lateral orbital gyrus. Analyses identified 1 ROC efficacy edge that was also associated with smoking lapse. Specifically, stronger rsFC from this cluster to the left rostral dorsal middle frontal gyrus and caudal lateral superior frontal gyrus was associated with better ROC efficacy and less hazard for smoking lapse (Fig. 3, Table 2). An additional 2 ROC efficacy edges from this cluster displaying notable associations with smoking lapse spanned connections to the precentral gyrus and superior parietal lobule ($p = 0.056$), and the superior and middle frontal gyrus ($p = 0.074$).

Left middle frontal gyrus seed cluster edges: The eighth selected cluster spanned the left caudal ventral middle frontal gyrus and caudal lateral superior frontal gyrus. Analyses identified 1 ROC efficacy edge that was also associated with smoking lapse. Specifically, stronger rsFC from this cluster to the right caudal

**Table 2.** Brain-behavior results: ROC Efficacy and smoking lapse edges.

| Anatomy | ROC Efficacy (partial cor.) | Smoking Lapse (cox regression) |
|---|---|---|
| ROC Efficacy and Smoking Lapse Edges | | |
| 1. L.Inferior Frontal Gyrus ↔ R.Precentral Gyrus | R = −0.403 [−0.237, −0.534], $p < 0.001$ | β = −2.985, HR = 0.051 [0.006, 0.420], $p = 0.006$ |
| 2. L.Inferior Frontal Gyrus ↔ L.Precentral Gyrus | R = −0.354 [−0.221, −0.476], $p < 0.001$ | β = −2.524, HR = 0.080 [0.012, 0.527], $p = 0.009$ |
| 3. L.Inferior Frontal Gyrus ↔ R.Postcentral Gyrus | R = −0.347 [−0.199, −0.462], $p < 0.001$ | β = −1.838, HR = 0.159 [0.027, 0.945], $p = 0.043$ |
| 4. L.Inferior Frontal Gyrus ↔ L.Paracentral Lobule | R = −0.322 [−0.204, −0.427], $p < 0.001$ | β = −1.788, HR = 0.167 [0.033, 0.848], $p = 0.031$ |
| 5. R.Dorsal Striatum ↔ R.Insula / Inferior Frontal Gyrus | R = −0.368 [−0.201, −0.515], $p < 0.001$ | β = −3.562, HR = 0.028 [0.002, 0.513], $p = 0.016$ |
| 6. R.Amygdala ↔ L.Postcentral / Precentral Gyrus | R = −0.353 [−0.178, −0.500], $p < 0.001$ | β = −2.344, HR = 0.096 [0.011, 0.829], $p = 0.033$ |
| 7. R.Amygdala ↔ L.Ventral Striatum | R = 0.380 [0.175, 0.552], $p < 0.001$ | β = 2.745, HR = 15.56 [1.927, 125.67], $p = 0.010$ |
| 8. R.Anterior Insula ↔ L.Middle Frontal Gyrus | R = −0.359 [−0.195, −0.500], $p < 0.001$ | β = −2.692, HR = 0.068 [0.012, 0.367], $p = 0.002$ |
| 9. L.Middle Frontal Gyrus ↔ R.Middle Temporal Gyrus / Caudal Hippocampus | R = −0.475 [−0.327, −0.609], $p < 0.001$ | β = −3.488, HR = 0.031 [0.003, 0.365], $p = 0.006$ |
| 10. L.Pre-Supplementary Motor Area ↔ L.Subgenual / Pregenual Cingulate | R = −0.366 [−0.222, −0.499], $p < 0.001$ | β = −2.294, HR = 0.101 [0.016, 0.637], $p = 0.015$ |
| Composite Score | | |
| Combined edge strength | R = −0.601 [−0.451, −0.707], $p < 0.001$ | β = −7.086, HR = 0.001 [0.000, 0.030], $p < 0.001$ |

ROC efficacy and smoking lapse edges, including their composite score, are described here. Statistical significance: $p$-value < 0.05 (two-tailed).

middle temporal gyrus and caudal hippocampus was associated with better ROC efficacy and less hazard for smoking lapse (Fig. 3, Table 2).

Left pre-supplementary motor area seed cluster edges: The ninth and final selected cluster spanned the left pre-supplementary motor area. Analyses identified 1 ROC efficacy edge that was also associated with smoking lapse. Specifically, stronger rsFC from this cluster to the left subgenual and pregenual cingulate gyrus was associated with better ROC efficacy and less hazard for smoking lapse (Fig. 3, Table 2). An additional 2 ROC efficacy edges from this cluster displaying notable associations with smoking lapse spanned connections to striatal regions ($p = 0.063$; $p = 0.063$).

*rsFC composite score*. In sum, the 10 ROC efficacy edges that were also associated with smoking lapse, resulted in a rsFC composite score that explained ROC efficacy (Fig. 4A) and smoking lapse (Fig. 4B **[top]**) better than any individual edge (Table 2). Specifically, the combined edge strength accounted for 36% of the variance in ROC efficacy (R = 0.601, 95% CI = −0.451 to −0.707, $p < 0.001$) and for every one-unit increase in edge strength, there was a 99% decrease in the hazard of smoking lapse (β = −7.086, SE = 1.825, HR = 0.001, 95% CI = 0.000–0.030, $p < 0.001$). No time-dependent effect of the composite score on smoking lapse was found ($p = 0.212$) suggesting the proportional hazards assumption was met. For descriptive purposes, k-means clustering (k = 2) was applied to this composite score to display differences in survival curves based on group combined edge strength (stronger [$N = 65$; M = 0.120, SD = 0.064] vs. weaker [$N = 148$; M = 0.002, SD = 0.038]). Follow-up descriptive analyses indicated that individuals with stronger expressions of these rsFC patterns exhibited less hazard of smoking lapse (β = −0.771, SE = 0.277, HR = 0.463, 95% CI = 0.269–0.797, $p = 0.005$) (Fig. 4B **[bottom]**).

## DISCUSSION

Results revealed four novel findings. First, worse ROC efficacy predicted a greater hazard of smoking lapse. Second, FC-MVPA procedures confirmed the extant hypothesis-driven literature [17, 18] by demonstrating that functional clusters in fronto-striatal-limbic circuitry were associated with ROC efficacy. Analyses also confirmed the extant data-driven literature [19] by demonstrating the importance of regions in sensory-motor and temporal-parietal circuitry. Third, follow-up SBC analyses, using selected FC-MVPA clusters, identified frontal-striatal-limbic edges as hypothesized, but also identified many edges consisting of connections between frontal-striatal-limbic circuitry and sensory-motor circuitry. Finally, of the 64 identified resting-state edges underlying ROC efficacy, 10 were associated with smoking lapse. Notably, these edges largely consisted of connections between fronto-striatal-limbic and sensory-motor circuitry and better behavioral outcomes were associated with stronger rsFC.

### Behavior

During the ROC task, self-reported cigarette craving was reduced during the reappraisal (SL) as compared to the now (SN) smoking cue condition, which replicates the extant literature [7–9, 11–13, 15]. Moreover, worse ROC efficacy (SL–SN) represented a greater hazard for smoking lapse, which is a novel contribution to the literature. In summary, study results suggest that ROC efficacy may be used for identifying individuals at greater risk for smoking re/lapse, and that providing ROC training may promote smoking cessation and help prevent relapse, as recently demonstrated by others [57, 58].

### Brain and behavior

The ROC efficacy FC-MVPA step identified 29 functional clusters displaying multivariate patterns of rsFC associated with ROC efficacy. Clusters spanned fronto-striatal-limbic circuitry, temporal-parietal circuitry, sensory-motor circuitry, and the prefrontal clusters were more dominant in the left hemisphere. These results are consistent with the extant fMRI BOLD response literature on ROC efficacy [17–19] and emotion regulation more broadly [18, 59]. In summary, study results suggest ROC efficacy comprises the whole-brain including fronto-striatal-limbic circuitry, that ROC efficacy and emotion regulation may share common neural mechanisms [18], and that the functional architecture of the resting brain is similar to that of the task-engaged brain [60].

The ROC efficacy SBC analysis step, using 9 ROC FC-MVPA-derived clusters, identified 64 resting-state edges underlying ROC efficacy, 10 of which also predicted the hazard for smoking lapse. Although the selected seed clusters were restricted to regions in fronto-striatal-limbic circuitry, the identified edges indicated that ROC efficacy and smoking lapse were largely predicted by connections between regions in fronto-striatal-limbic circuitry and sensory-motor circuitry, and thus not simply fronto-striatal-limbic circuitry itself as suggested by theory [55]. To the best of our knowledge, current mechanistic investigations into ROC

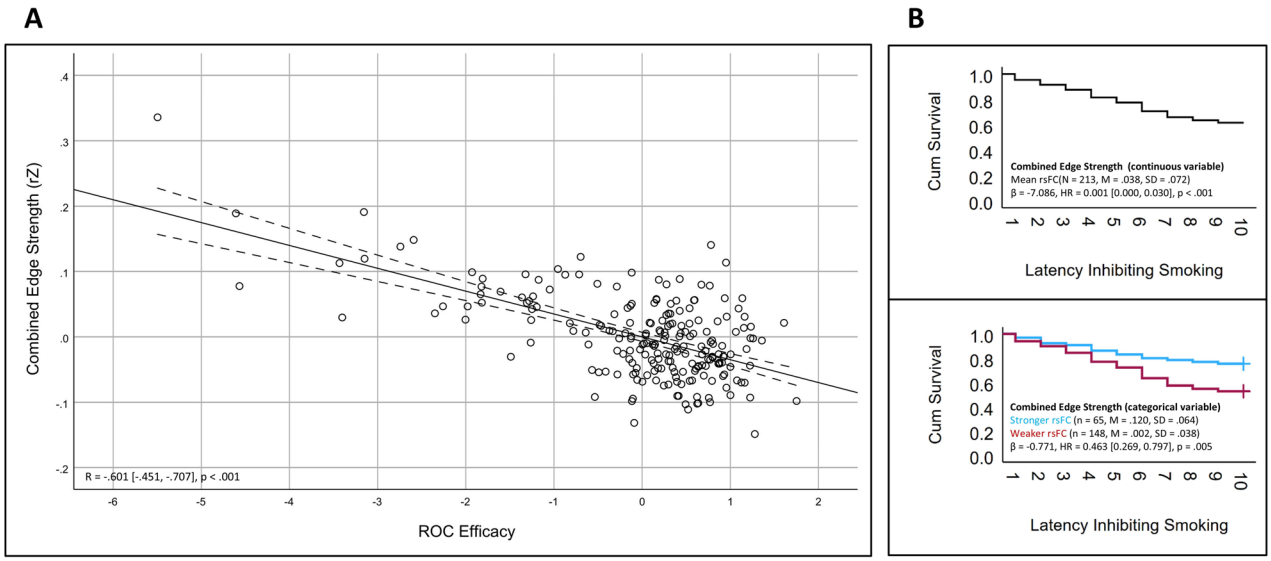


**Fig. 4 Brain-behavior results: ROC efficacy and smoking lapse edge composite score.** In sum, 10 ROC efficacy edges that were also associated with smoking lapse, resulted in a composite score that explained both ROC efficacy (**A**) and smoking lapse (**B top**) better than any individual edge (Table 2). Specifically, the combined edge strength accounted for 36% of the variance in ROC efficacy ($R = 0.601$, $p < 0.001$) and for every one-unit increase in edge strength, there was a 99% decrease in the hazard of smoking lapse ($\beta = -7.086$, $HR = 0.001$, $p < 0.001$). (**B bottom**) For descriptive purposes, k-means clustering ($k = 2$) was applied to this composite score to display differences in survival curves based on group rsFC strength (stronger vs. weaker). Individuals with stronger expressions of these rsFC patterns exhibited less hazard of smoking lapse ($\beta = -0.771$, $HR = 0.463$, $p = 0.005$). Statistical significance: $p$-value < 0.05 (two-tailed).

efficacy have been limited to BOLD response and thus have only been able to convey what brain regions are important. However, the present analyses extend the field's current working knowledge by informing how these brain regions communicate and support ROC efficacy. Edges underlying both ROC efficacy and smoking lapse are discussed below.

*Left inferior frontal gyrus seed cluster edges*. Provided the left inferior frontal gyrus supports language and motor functions [61–63], while the pre- and postcentral gyrus support sensory-motor functions [64], stronger rsFC between these regions may help improve motor control over smoking impulses driven by internal or external cues. Similar findings have been observed by others studying smoking relapse [65].

*Right dorsal striatum seed cluster edges*. Provided the dorsal striatum supports reward learning and habit formation [66], while the right inferior frontal gyrus support attentional control and response inhibition [67–70], stronger rsFC between these regions may help improve motor control over smoking impulses driven by internal or external cues. Similar findings have been observed by others studying smokers [27, 28, 30, 32], and other substance use disorders [24].

*Right amygdala seed cluster edges*. Provided the amygdala supports salience detection and emotion processing [61, 71, 72], while the ventral striatum supports reward learning [73] and the pre- and postcentral gyrus support sensory-motor processing [64], weaker rsFC between the amygdala and ventral striatum, yet stronger rsFC between the amygdala and pre- and post-central gyrus, may help rebalance the dynamics between bottom-up processing and top-down regulation of smoking cues. Specifically, weaker amygdala-striatum rsFC may help blunt drug-cue reactivity, while stronger amygdala-pre/postcentral gyrus rsFC may enable more efficient modulation over cue-induced cravings. These results are further supported by both animal [72, 74] and human [75–77] research.

*Right anterior insula seed cluster edges*. Provided the ventral anterior insula support socio-emotional processing [61, 69, 70], while the middle frontal gyrus support working memory and proactive inhibition [61, 67, 78], stronger rsFC may help keep attentional processes focused on future goals in contrast to internal sensations. Similar findings have been observed by others studying relapse in smokers [28, 32] and individuals with cocaine use disorder [79].

*Left middle frontal gyrus seed cluster edges*. Provided the middle frontal gyrus supports working memory and proactive inhibition [61, 67, 78], while the middle temporal gyrus and caudal hippocampus support memory [80, 81], stronger rsFC may be protective by strengthening mental representations of future goals when in the presence of smoking-related cues. Similar findings have been observed by others studying individuals with substance use disorders [82–84].

*Left pre-supplemental motor area seed cluster edges*. Provided the pre-supplementary motor area supports conflict monitoring and a variety of motor functions [61, 67, 85], while the subgenual/pregenual cingulate gyrus support negative valence and reward valuation [86], stronger rsFC may strengthen motor control over the influence of negative emotionality and reward expectancies on smoking behavior. Similar findings have been observed by others studying the effects of nicotine on acute abstinence in smokers [87].

*rsFC composite score*. Even though each of the 10 circuits described above predicted ROC efficacy and smoking lapse, when values were aggregated into a single composite score, associations with behavior were much stronger. This finding further reinforces the value of composite score approaches for predicting behavior [49]. Also, as suggested by others [88], composite score approaches are likely a more accurate representation of true brain-behavior relationships.

## Clinical relevance

Study findings have direct implications for future clinical research. Specifically, findings suggest that interventions that aim to improve ROC efficacy may help promote smoking abstinence, and possibly abstinence from other addictive substances. For example, future behavioral intervention trials may seek to

determine which specific ROC cognitive strategies are better for promoting abstinence (e.g., cognitive behavioral therapy [CBT] vs. mindfulness-oriented recover enhancement [MORE]) [89–93]; whereas future noninvasive brain stimulation trials may seek to stimulate novel targets to modulate craving [94], as identified in the present analyses, such as the inferior frontal gyrus or pre-supplemental motor area [33, 34]. Also, future studies may seek to replicate this work by computing combined edge strength for the edges identified here and using this information to predict relapse vulnerabilities in their own clinical sample. If replication is successful, then next steps may involve evaluating these circuits within the context of a treatment study and examining how neural circuitry changes correspond with behavioral changes.

### Strengths and weaknesses

Study strengths included investigating a relatively large sex-balanced sample of nicotine-dependent adult cigarette smokers and being the first study to triangulate associations between ROC efficacy, rsFC, and smoking lapse. However, the following weaknesses are acknowledged. First, this study pooled data across different sites and MRI scanners and parameters. Although imaging data adjusted for scanner effects and the processing pipeline was rigorous (mean subject framewise displacement was <0.2 mm), these differences may have allowed for undesired noise. Second, a subset of participant MRI data did not include the primary visual cortex or cerebellum due to missing coverage, and thus no inferences regarding these regions could be made. Third, regarding the SRT, this study investigated sated smokers and although significant effects on the ROC task were found, differences may have been more pronounced in abstinent smokers and the proportion of participants lapsing on the task may have been greater. Lastly, screening for mental and physical health problems was not based on structured clinical interviews, but rather on participant self-report. Despite these limitations, findings suggest that both ROC efficacy and underlying resting-state neural circuitry may inform prediction models of re/lapse vulnerabilities across an ecological valid and more inclusive representative sample of smokers, as well as potentially inform treatment targets for cessation interventions.

## DATA AVAILABILITY

The data supporting the conclusions of this article will be made available by the authors with reasonable request.

## CODE AVAILABILITY

The code for MRI analyses used in this article is publicly available (https://web.conn-toolbox.org/).

## REFERENCES

1. Ekhtiari H, Nasseri P, Yavari F, Mokri A, Monterosso J. Neuroscience of drug craving for addiction medicine: from circuits to therapies. Prog Brain Res. 2016;223:115–41.
2. Cofresí RU, Bartholow BD, Piasecki TM. Evidence for incentive salience sensitization as a pathway to alcohol use disorder. Neurosci Biobehav Rev. 2019;107:897–926.
3. Vafaie N, Kober H. Association of drug cues and craving with drug use and relapse: a systematic review and meta-analysis. JAMA Psychiatry. 2022;79:641–50.
4. Skinner MD, Aubin HJ. Craving's place in addiction theory: contributions of the major models. Neurosci Biobehav Rev. 2010;34:606–23.
5. Brody AL, Mandelkern MA, Olmstead RE, Jou J, Tiongson E, Allen V, et al. Neural substrates of resisting craving during cigarette cue exposure. Biol Psychiatry. 2007;62:642–51.
6. Volkow ND, Fowler JS, Wang GJ, Telang F, Logan J, Jayne M, et al. Cognitive control of drug craving inhibits brain reward regions in cocaine abusers. Neuroimage. 2010;49:2536–43.
7. Kober H, Mende-Siedlecki P, Kross EF, Weber J, Mischel W, Hart CL, et al. Prefrontal-striatal pathway underlies cognitive regulation of craving. Proc Natl Acad Sci USA. 2010;107:14811–6.
8. Hartwell KJ, Johnson KA, Li X, Myrick H, LeMatty T, George MS, et al. Neural correlates of craving and resisting craving for tobacco in nicotine dependent smokers. Addict Biol. 2011;16:654–66.
9. Zhao LY, Tian J, Wang W, Qin W, Shi J, Li Q, et al. The role of dorsal anterior cingulate cortex in the regulation of craving by reappraisal in smokers. PLoS ONE. 2012;7:e43598.
10. Wilson SJ, Sayette MA, Fiez JA. Neural correlates of self-focused and other-focused strategies for coping with cigarette cue exposure. Psychol Addict Behav. 2013;27:466–76.
11. Tabibnia G, Creswell JD, Kraynak T, Westbrook C, Julson E, Tindle HA. Common prefrontal regions activate during self-control of craving, emotion, and motor impulses in smokers. Clin Psychol Sci. 2014;2:611–9.
12. Ono M, Kochiyama T, Fujino J, Sozu T, Kawada R, Yokoyama N, et al. Self-efficacy modulates the neural correlates of craving in male smokers and ex-smokers: an fMRI study. Addict Biol. 2018;23:1179–88.
13. Ghahremani DG, Faulkner P, M Cox C, London ED. Behavioral and neural markers of cigarette-craving regulation in young-adult smokers during abstinence and after smoking. Neuropsychopharmacology. 2018;43:1616–22.
14. Suzuki S, Mell MM, O'Malley SS, Krystal JH, Anticevic A, Kober H. Regulation of craving and negative emotion in alcohol use disorder. Biol Psychiatry Cogn Neurosci Neuroimaging. 2020;5:239–50.
15. Kunas SL, Stuke H, Plank IS, Laing EM, Bermpohl F, Ströhle A. Neurofunctional alterations of cognitive down-regulation of craving in quitting motivated smokers. Psychol Addict Behav. 2022;36:1012–22.
16. Huang Y, Ceceli AO, Kronberg G, King S, Malaker P, Parvaz MA. et al. Association of Cortico-Striatal Engagement During Cue Reactivity, Reappraisal, and Savoring of Drug and Non-Drug Stimuli With Craving in Heroin Addiction. Am J Psychiatry. 2024;181:153–65.
17. Kober H, Mell MM. Neural mechanisms underlying craving and the regulation of craving. In S. J. Wilson (Ed.), The Wiley handbook on the cognitive neuroscience of addiction. Wiley Blackwell; 2015. pp 195–218.
18. Brandl F, Le Houcq Corbi Z, Mulej Bratec S, Sorg C. Cognitive reward control recruits medial and lateral frontal cortices, which are also involved in cognitive emotion regulation: a coordinate-based meta-analysis of fMRI studies. Neuroimage. 2019;200:659–73.
19. Koban L, Wager TD, Kober H. A neuromarker for drug and food craving distinguishes drug users from non-users. Nature Neuroscience. 2023;26:316–25.
20. Horien C, Greene AS, Constable RT, Scheinost D. Regions and connections: complementary approaches to characterize brain organization and function. Neuroscientist. 2020;26:117–33.
21. Elliott ML, Knodt AR, Ireland D, Morris ML, Poulton R, Ramrakha S, et al. What is the test-retest reliability of common task-functional MRI measures? new empirical evidence and a meta-analysis. Psychol Sci. 2020;31:792–806.
22. Elliott ML, Knodt AR, Cooke M, Kim MJ, Melzer TR, Keenan R, et al. General functional connectivity: shared features of resting-state and task fMRI drive reliable and heritable individual differences in functional brain networks. Neuroimage. 2019;189:516–32.
23. Sutherland MT, Carroll AJ, Salmeron BJ, Ross TJ, Stein EA. Insula's functional connectivity with ventromedial prefrontal cortex mediates the impact of trait alexithymia on state tobacco craving. Psychopharmacology. 2013;228:143–55.
24. Motzkin JC, Baskin-Sommers A, Newman JP, Kiehl KA, Koenigs M. Neural correlates of substance abuse: reduced functional connectivity between areas underlying reward and cognitive control. Hum Brain Mapp. 2014;35:4282–92.
25. Zanchi D, Brody AL, Montandon ML, Kopel R, Emmert K, Preti MG, et al. Cigarette smoking leads to persistent and dose-dependent alterations of brain activity and connectivity in anterior insula and anterior cingulate. Addict Biol. 2015;20:1033–41.
26. Stoeckel LE, Chai XJ, Zhang J, Whitfield-Gabrieli S, Evins AE. Lower gray matter density and functional connectivity in the anterior insula in smokers compared with never smokers. Addict Biol. 2016;21:972–81.
27. Yuan K, Yu D, Bi Y, Li Y, Guan Y, Liu J, et al. The implication of frontostriatal circuits in young smokers: a resting-state study. Hum Brain Mapp. 2016;37:2013–26.
28. Bi Y, Yuan K, Guan Y, Cheng J, Zhang Y, Li Y, et al. Altered resting state functional connectivity of anterior insula in young smokers. Brain Imaging Behav. 2017;11:155–65.
29. Wang C, Bai J, Wang C, von Deneen KM, Yuan K, Cheng J. Altered thalamo-cortical resting state functional connectivity in smokers. Neurosci Lett. 2017;653:120–5.
30. Wang C, Huang P, Shen Z, Qian W, Wang S, Jiaerken Y, et al. Increased striatal functional connectivity is associated with improved smoking cessation outcomes: a preliminary study. Addict Biol. 2021;26:e12919.
31. Dugré JR, Orban P, Potvin S. Disrupted functional connectivity of the brain reward system in substance use problems: a meta-analysis of functional neuroimaging studies. Addict Biol. 2023;28:e13257.
32. Zelle SL, Gates KM, Fiez JA, Sayette MA, Wilson SJ. The first day is always the hardest: functional connectivity during cue exposure and the ability to

resist smoking in the initial hours of a quit attempt. Neuroimage. 2017;151:24–32.
33. Upton S, Brown AA, Golzy M, Garland EL, Froeliger B. Right inferior frontal gyrus theta-burst stimulation reduces smoking behaviors and strengthens fronto-striatal-limbic resting-state functional connectivity: a randomized crossover trial. Frontiers in Psychiatry. 2023;14:1166912.
34. Upton S, Brown AA, Ithman M, Newman-Norlund R, Sahlem G, Prisciandaro JJ, et al. Effects of hyperdirect pathway theta-burst transcranial magnetic stimulation on inhibitory control, craving, and smoking in adults with nicotine dependence: a double-blind randomized crossover trial. Biol Psychiatry Cogn Neurosci Neuroimaging. 2023;8:1156–65.
35. Nieto-Castanon A. Brain-wide connectome inferences using functional connectivity multivariate pattern analyses (fc-MVPA). PLoS Comput Biol. 2022;18:e1010634.
36. Arnold Anteraper S, Guell X, D'Mello A, Joshi N, Whitfield-Gabrieli S, Joshi G. Disrupted cerebrocerebellar intrinsic functional connectivity in young adults with high-functioning autism spectrum disorder: a data-driven, whole-brain, high-temporal resolution functional magnetic resonance imaging study. Brain Connect. 2019;9:48–59.
37. Walsh MJM, Pagni B, Monahan L, Delaney S, Smith CJ, Baxter L, et al. Sex-related brain connectivity correlates of compensation in adults with autism: insights into female protection. Cereb Cortex. 2022;33:316–29.
38. Kelly E, Meng F, Fujita H, Morgado F, Kazemi Y, Rice LC, et al. Regulation of autism-relevant behaviors by cerebellar-prefrontal cortical circuits. Nat Neurosci. 2020;23:1102–10.
39. Kumar U, Arya A, Agarwal V. Altered functional connectivity in children with ADHD while performing cognitive control task. Psychiatry Res Neuroimaging. 2022;326:111531.
40. Katsumi Y, Moore M. Affective enhancement of episodic memory is associated with widespread patterns of intrinsic functional connectivity in the brain across the adult lifespan. Front Behav Neurosci. 2022;16:910180.
41. Froeliger B, McConnell PA, Bell S, Sweitzer M, Kozink RV, Eichberg C, et al. Association between baseline corticothalamic-mediated inhibitory control and smoking relapse vulnerability. JAMA Psychiatry. 2017;74:379–86.
42. Bell S, Froeliger B. Associations between smoking abstinence, inhibitory control, and smoking behavior: an fMRI study. Front Psychiatry. 2021;12:592443.
43. Brown AA, Upton S, Craig S, Froeliger B. Associations between right inferior frontal gyrus morphometry and inhibitory control in individuals with nicotine dependence. Drug Alcohol Depend. 2023;244:109766.
44. Kober H, Kross EF, Mischel W, Hart CL, Ochsner KN. Regulation of craving by cognitive strategies in cigarette smokers. Drug Alcohol Depend. 2010;106:52–5.
45. McKee SA. Developing human laboratory models of smoking lapse behavior for medication screening. Addict Biol. 2009;14:99–107.
46. Leeman RF, O'Malley SS, White MA, McKee SA. Nicotine and food deprivation decrease the ability to resist smoking. Psychopharmacology. 2010;212:25–32.
47. Whitfield-Gabrieli S, Nieto-Castanon A. Conn: a functional connectivity toolbox for correlated and anticorrelated brain networks. Brain Connect. 2012;2:125–41.
48. Friston K, Ashburner J, Kiebel S, Nichols T, Penny W. Statistical Parametric Mapping: The Analysis of Functional Brain Images. London: Academic Press; 2011.
49. Shen X, Finn ES, Scheinost D, Rosenberg MD, Chun MM, Papademetris X, et al. Using connectome-based predictive modeling to predict individual behavior from brain connectivity. Nat Protoc. 2017;12:506–18.
50. Yip SW, Scheinost D, Potenza MN, Carroll KM. Connectome-based prediction of cocaine abstinence. Am J Psychiatry. 2019;176:156–64.
51. Lichenstein SD, Scheinost D, Potenza MN, Carroll KM, Yip SW. Dissociable neural substrates of opioid and cocaine use identified via connectome-based modelling. Mol Psychiatry. 2021;26:4383–93.
52. Lin X, Zhu X, Zhou W, Zhang Z, Li P, Dong G, et al. Connectome-based predictive modelling of smoking severity in smokers. Addict Biol. 2022;27:e13242.
53. Garrison KA, Sinha R, Potenza MN, Gao S, Liang Q, Lacadie C, et al. Transdiagnostic connectome-based prediction of craving. Am J Psychiatry. 2023;180:445–53.
54. Taxali A, Angstadt M, Rutherford S, Sripada C. Boost in test-retest reliability in resting state fMRI with predictive modeling. Cereb Cortex. 2021;31:2822–33.
55. Koob GF, Volkow ND. Neurobiology of addiction: a neurocircuitry analysis. Lancet Psychiatry. 2016;3:760–73.
56. Zilverstand A, Huang AS, Alia-Klein N, Goldstein RZ. Neuroimaging impaired response inhibition and salience attribution in human drug addiction: a systematic review. Neuron. 2018;98:886–903.
57. Lopez RB, Ochsner KN, Kober H. Brief training in regulation of craving reduces cigarette smoking. J Subst Abuse Treat. 2022;138:108749.
58. Roos CR, Harp NR, Vafaie N, Gueorguieva R, Frankforter T, Carroll KM, et al. Randomized trial of mindfulness- and reappraisal-based regulation of craving training among daily cigarette smokers. Psychol Addict Behav. 2023;37:829–40.
59. Morawetz C, Bode S, Derntl B, Heekeren HR. The effect of strategies, goals and stimulus material on the neural mechanisms of emotion regulation: a meta-analysis of fMRI studies. Neurosci Biobehav Rev. 2017;72:111–28.
60. Smith SM, Fox PT, Miller KL, Glahn DC, Fox PM, Mackay CE, et al. Correspondence of the brain's functional architecture during activation and rest. Proc Natl Acad Sci USA. 2009;106:13040–5.
61. Wilcox CE, Pommy JM, Adinoff B. Neural circuitry of impaired emotion regulation in substance use disorders. Am J Psychiatry. 2016;173:344–61.
62. Bulut T. Domain-general and domain-specific functional networks of Broca's area underlying language processing. Brain Behav. 2023;13:e3046.
63. Rae CL, Hughes LE, Anderson MC, Rowe JB. The prefrontal cortex achieves inhibitory control by facilitating subcortical motor pathway connectivity. J Neurosci. 2015;35:786–94.
64. Kropf E, Syan SK, Minuzzi L, Frey BN. From anatomy to function: the role of the somatosensory cortex in emotional regulation. Braz J Psychiatry. 2019;41:261–9.
65. Addicott MA, Sweitzer MM, Froeliger B, Rose JE, McClernon FJ. Increased functional connectivity in an insula-based network is associated with improved smoking cessation outcomes. Neuropsychopharmacology. 2015;40:2648–56.
66. Lipton DM, Gonzales BJ, Citri A. Dorsal striatal circuits for habits, compulsions and addictions. Front Syst Neurosci. 2019;13:28.
67. Jahanshahi M, Obeso I, Rothwell JC, Obeso JA. A fronto-striato-subthalamic-pallidal network for goal-directed and habitual inhibition. Nat Rev Neurosci. 2015;16:719–32.
68. Hartwigsen G, Neef NE, Camilleri JA, Margulies DS, Eickhoff SB. Functional segregation of the right inferior frontal gyrus: evidence from coactivation-based parcellation. Cereb Cortex. 2019;29:1532–46.
69. Kurth F, Zilles K, Fox PT, Laird AR, Eickhoff SB. A link between the systems: functional differentiation and integration within the human insula revealed by meta-analysis. Brain Struct Funct. 2010;214:519–34.
70. Uddin LQ, Nomi JS, Hébert-Seropian B, Ghaziri J, Boucher O. Structure and function of the human insula. J Clin Neurophysiol. 2017;34:300–6.
71. Volkow ND, Wang GJ, Tomasi D, Baler RD. Unbalanced neuronal circuits in addiction. Curr Opin Neurobiol. 2013;23:639–48.
72. Janak PH, Tye KM. From circuits to behaviour in the amygdala. Nature. 2015;517:284–92.
73. Everitt BJ, Robbins TW. From the ventral to the dorsal striatum: devolving views of their roles in drug addiction. Neurosci Biobehav Rev. 2013;37:1946–54.
74. Puaud M, Higuera-Matas A, Brunault P, Everitt BJ, Belin D. The basolateral amygdala to nucleus accumbens core circuit mediates the conditioned reinforcing effects of cocaine-paired cues on cocaine seeking. Biol Psychiatry. 2021;89:356–65.
75. Peters J, Miedl SF, Büchel C. Elevated functional connectivity in a striatal-amygdala circuit in pathological gamblers. PLoS ONE. 2013;8:e74353.
76. Aloi J, McCusker MC, Lew BJ, Schantell M, Eastman JA, Frenzel MR, et al. Altered amygdala-cortical connectivity in individuals with *Cannabis* use disorder. J Psychopharmacol. 2021;35:1365–74.
77. Belleau EL, Ehret LE, Hanson JL, Brasel KJ, Larson CL, deRoon-Cassini TA. Amygdala functional connectivity in the acute aftermath of trauma prospectively predicts severity of posttraumatic stress symptoms. Neurobiol Stress. 2020;12:100217.
78. Genon S, Li H, Fan L, Müller VI, Cieslik EC, Hoffstaedter F, et al. The right dorsal premotor mosaic: organization, functions, and connectivity. Cereb Cortex. 2017;27:2095–110.
79. Zhai T, Salmeron BJ, Gu H, Adinoff B, Stein EA, Yang Y. Functional connectivity of dorsolateral prefrontal cortex predicts cocaine relapse: implications for neuromodulation treatment. Brain Commun. 2021;3:fcab120.
80. Xu J, Lyu H, Li T, Xu Z, Fu X, Jia F, et al. Delineating functional segregations of the human middle temporal gyrus with resting-state functional connectivity and coactivation patterns. Hum Brain Mapp. 2019;40:5159–71.
81. Koban L, Lee S, Schelski DS, Simon MC, Lerman C, Weber B, et al. An fMRI-based brain marker of individual differences in delay discounting. J Neurosci. 2023;43:1600–13.
82. Liang X, He Y, Salmeron BJ, Gu H, Stein EA, Yang Y. Interactions between the salience and default-mode networks are disrupted in cocaine addiction. J Neurosci. 2015;35:8081–90.
83. Li Q, Liu J, Wang W, Wang Y, Li W, Chen J, et al. Disrupted coupling of large-scale networks is associated with relapse behaviour in heroin-dependent men. J Psychiatry Neurosci. 2018;43:48–57.
84. Zhang R, Volkow ND. Brain default-mode network dysfunction in addiction. Neuroimage. 2019;200:313–31.
85. Li W, Qin W, Liu H, Fan L, Wang J, Jiang T, et al. Subregions of the human superior frontal gyrus and their connections. Neuroimage. 2013;78:46–58.
86. Rolls ET. The cingulate cortex and limbic systems for action, emotion, and memory. Handb Clin Neurol. 2019;166:23–37.

87. Hong LE, Gu H, Yang Y, Ross TJ, Salmeron BJ, Buchholz B, et al. Association of nicotine addiction and nicotine's actions with separate cingulate cortex functional circuits. Arch Gen Psychiatry. 2009;66:431–41.
88. Westlin C, Theriault JE, Katsumi Y, Nieto-Castanon A, Kucyi A, Ruf SF, et al. Improving the study of brain-behavior relationships by revisiting basic assumptions. Trends Cogn Sci. 2023;27:246–57.
89. Verdejo-Garcia A, Rezapour T, Giddens E, Khojasteh Zonoozi A, Rafei P, Berry J, et al. Cognitive training and remediation interventions for substance use disorders: a Delphi consensus study. Addiction. 2023;118:935–51.
90. Froeliger B, Mathew AR, McConnell PA, Eichberg C, Saladin ME, Carpenter MJ, et al. Restructuring reward mechanisms in nicotine addiction: a pilot fMRI study of mindfulness-oriented recovery enhancement for cigarette smokers. Evid Based Complement Alternat Med. 2017;2017:7018014.
91. Garland EL, Howard MO, Priddy SE, McConnell PA, Riquino MR, Froeliger B. Mindfulness training applied to addiction therapy: insights into the neural mechanisms of positive behavioral change. Neuroscience and Neuroeconomics. 2016;5:55–63.
92. Germeroth LJ, Carpenter MJ, Baker NL, Froeliger B, LaRowe SD, Saladin ME. Effect of a brief memory updating intervention on smoking behavior: a randomized clinical trial. JAMA Psychiatry. 2017;74:214–23.
93. Palmer AM, Carpenter MJ, Baker NL, Froeliger B, Foster MG, Garland EL, et al. Development of two novel treatments to promote smoking cessation: Savor and retrieval-extinction training pilot clinical trial findings. Exp Clin Psychopharmacol. 2024;32:16–26.
94. Rose JE, McClernon FJ, Froeliger B, Behm FM, Preud'homme X, Krystal AD. Repetitive transcranial magnetic stimulation of the superior frontal gyrus modulates craving for cigarettes. Biol Psychiatry. 2011;70:794–9.

## AUTHOR CONTRIBUTIONS

SU: Conceptualization, Methodology, Software, Validation, Formal Analysis, Investigation, Data Curation, Writing – Original Draft, Writing – Review & Editing, Visualization, Project Administration. BF: Resources, Investigation, Data Curation, Writing – Review & Editing, Supervision, Project Administration, Funding Acquisition.

## FUNDING

This work was supported by the National Institutes of Health (NIH)/National Institute on Drug Abuse (NIDA) (Grant Nos. R01DA038700, R01DA048094, and UG3DA048510 [BF]) and the NIH/National Institute of Alcohol Abuse and Alcoholism (NIAAA) (Grant No. T32 AA013526 [SU; principal investigator, Dr. Dennis McCarthy]).

## COMPETING INTERESTS

The authors declare no competing interests.

## ETHICS APPROVAL AND INFORMED CONSENT

The studies involving human participants were reviewed and approved by the Institutional Review Board of the University of Missouri–Columbia and the Medical University of South Carolina. The patients/participants provided their written informed consent to participate in this study. All methods were performed in accordance with the relevant guidelines and regulations.

## ADDITIONAL INFORMATION

**Supplementary information** The online version contains supplementary material available at https://doi.org/10.1038/s41398-025-03319-1.

**Correspondence** and requests for materials should be addressed to Spencer Upton.

**Reprints and permission information** is available at http://www.nature.com/reprints

**Publisher's note** Springer Nature remains neutral with regard to jurisdictional claims in published maps and institutional affiliations.